This is a previous version of the article published in ACS Applied Materials & Interfaces. 2024, 16(4): 4540-4549. https://doi.org/10.1021/acsami.3c14208

Boosting Oxygen Reduction at Pt(111)|Proton Exchange Ionomer Interfaces through Tuning the Microenvironment Water Activity

Yu-Jun Xu,[1] Lu-Lu Zhang,[1] Wei Chen,[1] Hao-Wen Cui,[1] Jun Cai,[1] Yan-Xia Chen,*[,1] Juan M. Feliu[2] and Enrique Herrero*[,2]

[1]*Hefei National Research Center for Physical Sciences at Microscale, Department of Chemical Physics, University of Science and Technology of China, Hefei, 230026, China*

[2]*Instituto de Electroquímica, Universidad de Alicante, Apdo. 99, Alicante, E-03080, Spain*

Abstract Proton exchange ionomer's structure and the wetting conditions have a great impact on the microenvironment at the three-phase interphases in the membrane electrode assemblies(MEAs) of polymer electrolyte membrane fuel cells (PEMFCs), which can significantly influence the electrode kinetics. Herein, by using the Pt(111)|X ionomer interface as a model system (X= Nafion, Aciplex, D72), we found that higher drying temperature lowers the onset potential for sulfonate adsorption and lowers apparent current for ORR, while the current wave for OH_{ad} drops and shifts positively. Surprisingly, the intrinsic ORR activity is higher after proper correction of the blocking effect of Pt active sites by sulfonate adsorption and the PTFE skeleton. These results are well explained by the reduced water activity at the interfaces obtained after ionomer / PTFE coating, according to the mixed potential effect. Implications on how to prepare MEAs with improved ORR activity are provided.

Keywords: Pt(111); ionomer; adsorption; water activity; oxygen reduction reaction;

TOC Graphic:

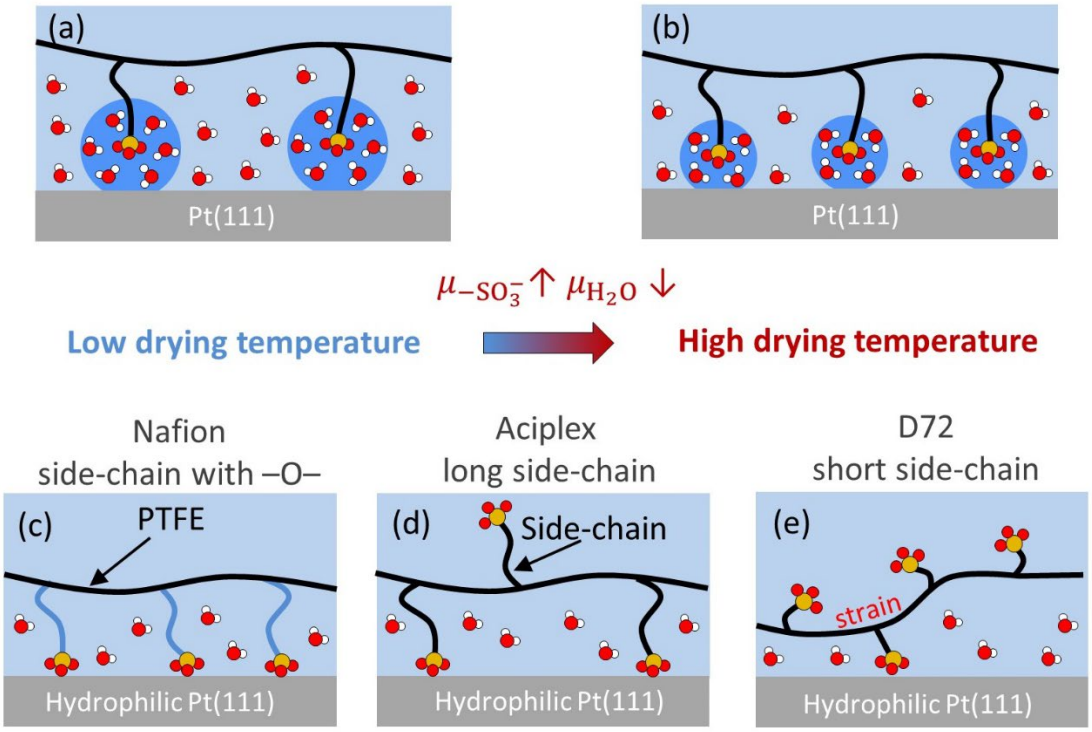
(a)
Pt(111)
(b)
Pt(111)
$\mu_{-SO_3^-}\uparrow \mu_{H_2O}\downarrow$
Low drying temperature
High drying temperature
Nafion
side-chain with –O–
Aciplex
long side-chain
D72
short side-chain
(c)
PTFE
Hydrophilic Pt(111)
(d)
Side-chain
Hydrophilic Pt(111)
(e)
strain
Hydrophilic Pt(111)

1. Introduction

Proton exchange membrane fuel cells (PEMFCs) are one of the most promising power sources for automobiles, portable electronics, and other industrial and civil applications.[1] The composition and structure of the membrane electrode assemblies (MEAs) in the PEMFCs determine the cell performance and the operating energy efficiency.[2, 3] The catalyst layers in the MEAs of PEMFCs are the places where electrode reactions take place. Optimized performance of the PEMFCs can only be realized using MEAs with the right structure, catalysts amount and composition, proton exchange ionomer, and supporting materials. To ensure that, the catalytic activity, the proton, and electronic conductivity as well as the mass transport for both reactants and products have to be optimized simultaneously. Major improvements have been achieved in the past decades by optimizing the catalysts, supports, and ionomer. Thus, Pt-based nanoparticles (NPs) with optimized electrocatalytic activity have been developed,[4-6] and carbon supports with optimum composition, particle size, and electronic conductivity have been synthesized.[7, 8] Perfluorosulfonic acid (PFSA) ionomers, consisting of hydrophobic perfluoro-alkyl-chain with fully perfluorinated ether side-chain terminated by hydrophilic -SO_3H anions, have been well confirmed to act as good proton conductors as well as binders for the nano-catalysts and the carbon support.[9-11] The humidity degree of the ionomers as well as the specific adsorption of sulfonate on Pt-based nano-catalysts dramatically alter the electrocatalysts' mass activity.[12, 13]

Mitigation of the sulfonate adsorption on the nano-catalysts while maintaining good proton conductivity and mass transport conditions in the PEMFCs is a prerequisite in order to improve cell performance. To this end, information on how the molecular structure of the ionomer and the conditions for preparing the MEAs affect the adsorption behavior of the sulfonate group as well as how sulfonate adsorbates impact the kinetics of fuel cell reactions will be crucial for the development of more efficient fuel cells. A diminution in the structural complexity of the interface for practical MEAs would be very helpful to reach these goals. One approach is the use of model systems composed of well-defined single crystalline Pt(hkl)|ionomer interfaces. Despite that, the research on this type of interface is still very limited. Previous studies have clearly shown that sulfonate adsorption at the Pt|ionomer interface gives rise to the appearance of well-defined peaks in the double-layer region of the cyclic voltammograms (CVs).[14-17] For ionomers with longer side-chain, the coverage of sulfonate adsorption is found to be higher, which correlates well with a stronger inhibition of kinetics for oxygen reduction reaction (ORR).[18, 19] Furthermore, the adsorption of the sulfonate group is confirmed to be enhanced with the drying of the ionomer, as indicated by a negative shift of the onset potential for its adsorption.[20] One recent study suggests that ionomer with ring-structured backbone can deliver higher power density, probably due to the suppression of densely layered folding of polymer backbones near the catalyst surfaces, which mitigates the poisoning of the catalyst by sulfonate groups and increases oxygen solubility.[21]

Furthermore, some ionic liquids (IL), tetrahexylammonium cations, cyclohexanol, or ionic covalent organic framework (COF) nanosheets present at the Pt catalyst|Nafion interface are found to prevent the specific adsorption of sulfonate and can act as promising modifiers to improve ORR kinetics.[22-26] Although a consensus on the deactivation of the electrocatalysis by sulfonate adsorption has been reached, information on the dependence of sulfonate adsorption on the humidity degree as well as on the extent to which ORR is inhibited due to sulfonate adsorbate is scarce.[20]

Besides blocking active sites, sulfonate adsorbate may induce more complex electrostatic double-layer effects or electronic effects at the electrocalaysts|ionomer interface. Furthermore, the change of the humidity degree not only regulates sulfonate adsorption but also affects OH_{ad} adsorption and the chemical potential as well as the hydrogen bond network of water at the catalsyt|ionomer interfaces. The latter has been suggested to significantly alter the ORR kinetics.[20, 27, 28] To unveil the roles of such variables, we have systematically investigated the Pt(111)|ionomer interfaces by using Nafion, Aciplex, and D72 as proton exchange ionomers (Fig.1). Using Nafion as the reference ionomer, the roles of the hydrophobicity and the length of the surface chain will be investigated. Aciplex has a similar equivalent molecular weight and side-chain length while it is slightly more hydrophobic than Nafion due to the lack of the ether group in the middle of the side chain. D72 has a shorter side chain and a lower equivalent molecular weight. The effect of the drying temperature on the adsorption behavior of sulfonate and OH_{ad} as well as ORR kinetics at the Pt(111)|ionomers interfaces will be also discussed. The drying temperature will change the humidity degree of the ionomer, which alters the water activity as well as the electrostatic double-layer effect induced by sulfonate adsorbate.[29, 30] The results obtained here will definitively serve to develop strategies on how to boost PEMFCs performance by exploiting the positive effect of a low water activity and how to mitigate the adverse effect of sulfonate adsorption.

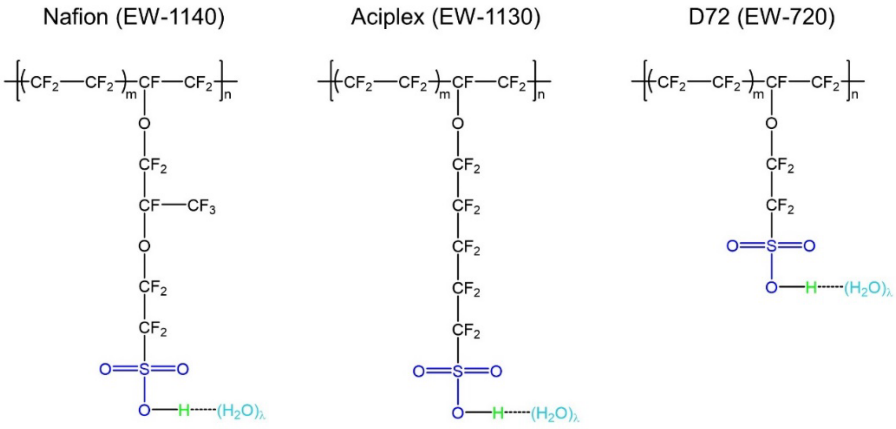

Fig. 1 Chemical structure of different proton exchange ionomers used in the construction of Pt(111)|ionomer interface in this study.

2. Experiment

The working electrode (WE), i.e., the Pt(111) single crystal electrode, is fabricated from a small metal bead using Clavilier's method.[31-33] The ionomer-coated Pt(111) electrode is prepared with Aciplex (Asahi KASEI, EW=1130 g/eq), Nafion (DuPont, EW=1140 g/eq), and Aquivion Dispersion D72-25BS (Solvay, EW=720 g/eq, Fig.1), according to the procedure described in reference [16]. The electrochemical experiments are conducted in a conventional three-electrode glass cell at room temperature. The counter electrode (CE) is Pt wire and the reference electrode (RE) is Ag/AgCl (with saturated KCl solution) electrode. All the potentials quoted in this work are against the reversible hydrogen electrode (RHE). The electrode potential is controlled by an Autolab 302N potentiostat. Current densities are calculated using the active area of the electrode, which, for single-crystal electrodes, coincides with the geometrical area. A 90% ohmic resistance compensation is automatically applied by the potentiostat using the positive feedback option. Solutions of 0.1 M $HClO_4$, 0.05 M H_2SO_4, and 0.1 M $HClO_4$+x M H_2SO_4 are prepared using perchloric acid (70%, Sigma Aldrich), sulfuric acid (96%, Sigma Aldrich), and ultra-pure water (18.2 MΩ, from Milli Q water system). During the experiments, solutions were deaerated using Argon (99.999%, the Linde Group, China). For the ORR experiments, hanging meniscus rotation disk experiments were carried out in oxygen (99.999%, the Linde Group, China) saturated solutions. The electrode rotation rate is controlled by modulated rotator (Hokuto Denko Ltd.).

3. Results and discussion

3.1 Impact of drying temperature on sulfonate and OH adsorption at Pt(111)|Aciplex interfaces

Fig.2a shows the cyclic voltammograms (CVs) of the Aciplex thin film-coated Pt(111) model interface prepared under different drying temperatures. For comparison, the CV of the unmodified Pt(111) electrode in 0.1 M $HClO_4$ is also included in Fig.2a. To better understand how the interfacial structure affects the ORR, control experiments in 0.1 M $HClO_4$, 0.05 M H_2SO_4 as well as 0.1 M $HClO_4$ + x M H_2SO_4 (x= 10^{-4}, 10^{-5} and 4×10^{-6}) have also been carried out (Fig. S1a). The CV of the unmodified Pt(111) electrode in $HClO_4$ solutions can be divided into three potential regions. The current signal between 0.05 and 0.4 V is mainly associated with the under-potential deposition of H (H_{UPD}) on the Pt surface. In the negative scan direction, H_{UPD} is formed from the proton discharge whereas the current in the positive scan direction corresponds with the oxidative removal of H_{UPD}. This region is followed by a double layer (DL) region from 0.4 to 0.6 V and then by the reversible OH adsorption region from 0.6 to 0.95 V. In acidic media, the adsorption/desorption of OH comes from water oxidation/reduction processes. For the Pt(111)|Aciplex interface prepared with a drying temperature of 120 °C, the current signals for H_{UPD} in the potential region from 0.4 to 0.25 V are slightly smaller than those obtained for the unmodified Pt(111) electrode. The overall integral charge is ca. 12% lower than that of the Pt(111)|0.1 M $HClO_4$ interface. The diminution of the hydrogen charge in this region can have two different origins. First, it could be due to a diminution of the active sites at the Pt(111) surface due to physical blocking by the polytetrafluoroethylene (PTFE) skeleton in Aciplex. Another possible explanation for this is the change in the water activity due to the presence of the ionomer at the interface. Similar displacement of the H_{UPD} region to more negative potentials has been observed as solution pH increases, revealing the role of the water structure in the H adsorption process.[34]

In the DL region, there is a small current wave due to the irreversible adsorption/desorption of the sulfonate group. The coverage of sulfonate adsorbate can be estimated from the charge flowing through the electrode|electrolyte interface, which is found to be approximately between 0.051-0.067 ML, depending on the drying temperature. This value is comparable to the coverage obtained in the negative scan direction for the Pt(111) electrode in 0.1 M $HClO_4$ + 10^{-5} M H_2SO_4. Under these conditions, the formation of the sulfate adsorbed layer is controlled by diffusion and thus the coverage is significantly smaller than the saturation coverage (0.20 ML). This coverage is obtained for higher concentrations, as shown for the sulfate adlayer formed at the Pt(111)|0.05 M H_2SO_4 interface (Fig.S1).[35-37] Furthermore, it is found that the current wave for sulfonate adsorption in the positive scan direction is ca. 60 mV more positive than that for its desorption in the negative scan. This indicates that the sulfonate adsorption/desorption process at the Pt(111)|Aciplex interface is rather irreversible, in contrast to the reversible sulfate adsorption at the Pt(111)|H_2SO_4 aqueous solution interface.[35, 36] All these imply that the local environment

of the sulfonate group within the hydrophilic channel of ionomer differs greatly from that of (bi-)sulfate anions in an aqueous electrolyte. Probably, the limited availability of water molecules in the channels disfavors the sulfonate desorption. It should be highlighted that the sulfonate groups are stabilized by the interaction with water molecules.

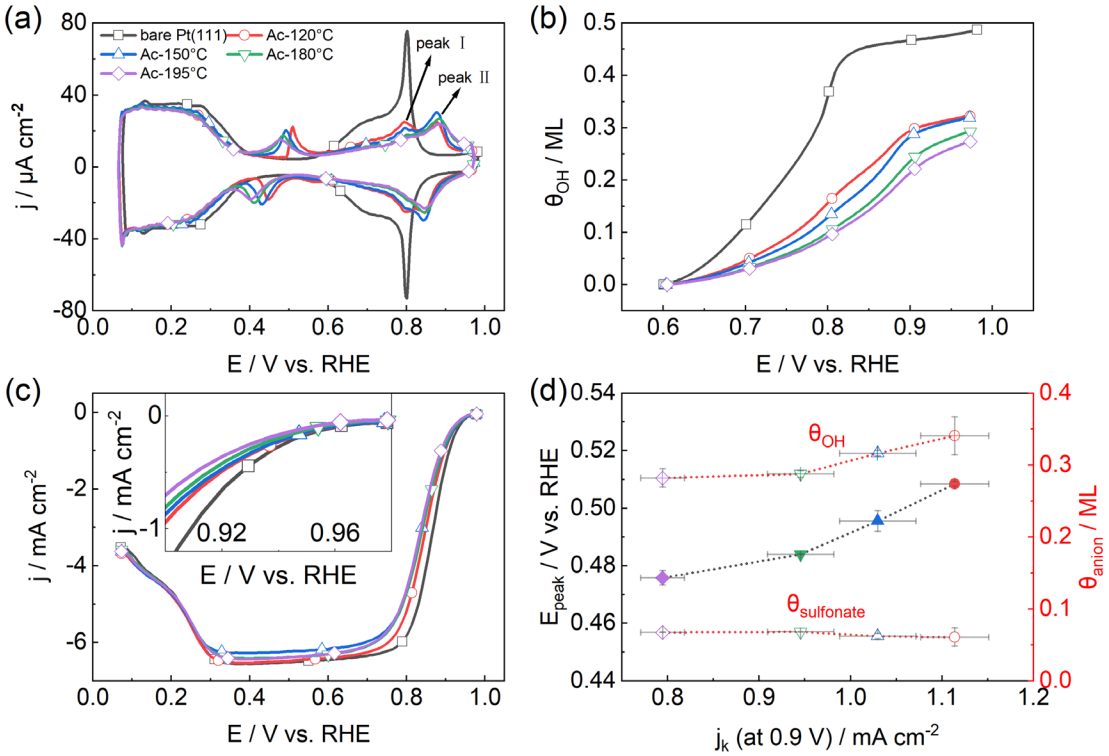

Fig. 2 (a) CVs for Pt(111)|Aciplex film electrodes with a thickness of ca. 100 nm prepared under different drying temperatures. (b) Coverage of adsorbed OH (θ_{OHad}, after the correction of double-layer charging current) as a function of the applied potential. (c) Polarization curves for ORR recorded in the positive scan direction. Inset: detailed view of the kinetic region of the ORR polarization curves. (d) Peak potentials for sulfonate adsorption (black) and the overall coverage of OH_{ad} and sulfonate (red), as a function of j_k for the ORR at 0.9 V on the Pt(111)|Aciplex film electrodes with different drying temperatures. For comparison, the CV and the j-E curve for the ORR on the unmodified Pt(111) electrode are also included in (a) and (c). Electrolyte: 0.1 M $HClO_4$, scan rate: 50 mV/s. For the ORR experiments, the rotation rate is 1600 rpm.

When the Aciplex ionomer is at the Pt(111) surface, the current wave for OH_{ad} formation from water oxidation at Pt(111) splits into two peaks. Peak I (at ca. 0.8 V) appears at the same potential as the sharp peak observed on the unmodified Pt(111), whereas peak II appears at higher potentials (centered at ca. 0.88 V), in agreement with previous reports on the Pt|ionomer and Pt|trifluoromethanesulfonic acid interfaces.[18, 19, 38] The adsorption and desorption peaks for OH are also slightly irreversible compared to those observed for the Pt(111)|$HClO_4$ aqueous solution interface (Fig.2a). The coverages of OH_{ad} at the Pt(111)|Aciplex interface as a function of the applied potential are shown in Fig.2b. These coverages have been obtained from the

integration of CVs after correction of the double layer charging current between 0.6 and 0.95 V. When compared to the unmodified Pt(111) electrode, the overall OH_{ad} coverage at Pt(111)|Aciplex interface is ca. 33-43% smaller. The differences in the OH adsorption region for the modified electrodes can be explained by the presence of the ionomer. First, the appearance of peak II should be related to the different chemical environments at the interface. The chemical potential of the water molecules within the hydrophilic channel of the ionomer should be slightly smaller than that in the aqueous electrolyte, either due to the less abundance or stronger interaction among those water molecules, as well as between water molecules and sulfonate groups within the hydrophilic channel. Also, the presence of adsorbed sulfonate groups on the surface (at E>0.5 V) can give rise to lateral repulsions. Both facts will hinder OH_{ad} formation and thus this process appears at higher potentials. This is supported by the slight positive shift of the OH_{ad} adsorption peak at the Pt(111)|0.1 M $HClO_4$ + 10^{-5} M H_2SO_4 interface (Fig.S1a). The inhibition of the current wave for peak I and the reduction of the overall OH_{ad} adsorption charge are probably the results of the blocking of the active sites at the Pt(111) surface by adsorbed sulfonate and the PTFE skeleton in contact with the Pt(111) surface.[37] The decrease of the wettability of the Pt(111) surface is ca. 12% as estimated from the reduction of H_{UPD} charge as a result of the blockage by the PTFE skeleton in the Aciplex ionomer. The blocking of Pt(111) surface by the sulfonate group is ca. 23-30% as estimated from the charge involved in sulfonate adsorption, assuming that one sulfonate occupies three Pt atoms. Since the overall charge for OH_{ad} formation has dropped ca. 33-43% with the introduction of Aciplex into the Pt(111) interface, all these facts reveal that the reduced OH_{ad} coverage is mainly resulting from the blocking of the active sites by the ionomer.

With the increase of the drying temperature used for the preparation of the Aciplex thin film-covered Pt(111) electrode, the current wave in the H_{UPD} region does not show significant changes. This further confirms that the smaller H_{UPD} current wave compared to that of Pt(111)|0.1 M $HClO_4$ interface can be mainly attributed to the blocking effect from the PTFE skeleton in the ionomer. The structure of the PTFE skeleton near the Pt(111) surface is not sensitive to the change of the drying temperature used for the preparation of the Pt|Aciplex interface, since the water content diminishes with the increasing drying temperature. With the increase of the drying temperature from 120 °C to 195 °C, the coverage of sulfonate adsorbate is found to increase from ca. 0.051 ML to ca. 0.067 ML, while the peak potentials for sulfonate adsorption shifts negatively from 0.5 V to 0.47 V. This trend is the same as the negative shift of sulfonate adsorption peaks during the dry-gas flow in a solid-state cell with Pt|Nafion interface.[20] Also, a similar negative shift of sulfate adsorption peak at the Pt group metal|aqueous solution interface is observed with the increase of

the concentration of sulfuric acid or sulfate anions in the bulk solution.[35, 39]

The negative shift of sulfonate adsorption potential with increasing the drying temperature used for the preparation of the Pt(111)|ionomer interface is likely a result of the change in the local environment of the hydrophilic region within the ionomer. The higher the annealing temperature is, the less content of water within the membrane will be (Fig. 4a, b). This leads to a less favorable local environment for the sulfonate group or an apparent higher sulfonate concentration in the hydrophilic region in the membrane. As a result, the chemical potential of the sulfonate group within the thin film increases. Since the equilibrium potential of sulfonate adsorption depends on the difference in its chemical potential before and after its adsorption, hence sulfonate adsorption starts at a lower potential when the drying temperature becomes higher. The slight broadening of the sulfonate adsorption peak with the increase in drying temperature is probably a result of the decrease in water content within the hydrophilic channel of the ionomer. The irreversibility of the adsorption/desorption process also increases with the drying temperature, indicating that once sulfonate is being adsorbed, its desorption will be more difficult. This can be rationalized by the fact that the binding to the Pt surface is stronger and fewer water molecules are within the hydrophilic channel of the ionomer to stabilize the desorbed sulfonate groups.

With the increase of the drying temperature, the current wave of peak I for the formation of OH_{ad} diminishes, the fragment of peak II with E<0.9 V decreases while the part with E>0.9 V increases. The difference in water environment at Pt(111)|Aciplex interface from that of Pt(111)|0.1 M $HClO_4$, as well as the drying temperature-induced change of water content within the hydrophilic channel of Aciplex, is probably the dominating factor for the change of the adsorption wave for OH_{ad} formation. The higher the drying temperature used for preparing the Pt|Aciplex interfaces, the lower the water content within the ionomer (Fig. 4a, b). This renders a smaller chemical potential and a positive shift of the OH_{ad} adsorption peak. Besides, other factors such as the slight increase of sulfonate coverage as well as the change of its adsorption properties (as evidenced by the broadening of its adsorption peak) may also lead to the decrease of the current wave for peak I and II as well as the slight positive shift of peak II (see SI and further discussions below).

The base CVs at the Pt(111)|Nafion and Pt|D72 interfaces prepared with different drying temperatures are shown in Fig.S2a, S3a. They are similar to those recorded at Pt(111)|Aciplex interfaces. For the Pt|ionomer interfaces prepared using the same drying temperature, sulfonate coverage increases in the order of Pt(111)|D72 < Pt(111)|Aciplex < Pt(111)|Nafion (Fig.3, S4a). The interface structure of Pt(111)|X (Nafion, Aciplex, D72) is shown in Fig. 4c, d, and e, which indicates that sulfonate coverage depends not only on the side-chain length but also on the presence or absence of ether group in the side-chain. The sulfonate group at the end of the hydrophilic side-chain with the ether group tends to be close to the hydrophilic Pt(111) electrode since this side-chain is more flexible in the hydrophilic channels of the ionomer.[40-42] As for Pt(111)|D72, the short side-chain strains the PTFE main chain when sulfonate is adsorbed, which hinders D72 sulfonate group adsorption. This is in good agreement with the literature, reporting that the poisoning effect by sulfonate adsorbate is smaller in ionomers with shorter side-chain.[18] Higher sulfonate coverage at Pt(111)|Nafion is followed by a much smaller current wave for peak I and a more dominating current peak II for OH_{ad} adsorption (Fig.3a, S4a).

3.2 Impact of humidity degree on ORR kinetics at Pt(111)|proton exchange ionomer Interfaces

The polarization curves for ORR at the Pt(111)|Aciplex interfaces prepared with different drying temperatures are shown in Fig.2c. For comparison the j-E curve for ORR at bare Pt(111) in O_2 saturated 0.1 M $HClO_4$ under identical conditions is also included. As the drying temperature increases, a diminution of the limiting current can be observed. This decrease cannot be attributed to the reduction of the active area due to the partial blocking of the surface by the PTFE chain, since the limiting current depends on the geometrical area. Thus, it should be assigned to the hindrance of O_2 diffusion in the interface as the water content diminishes. On the other hand, in the region where the ORR current is kinetically controlled, a diminution of the current at constant potentials is observed with the introduction of the proton exchange ionomer (Fig.2c). The extent of this inhibition augments with the increasing drying temperature for preparing the Aciplex thin film. The temperature dependence of the polarization curves for ORR at the Pt(111)|Nafion and Pt(111)|D72 interfaces prepared with different drying temperatures is shown in Fig.S2c and Fig.S3c. They are similar to those recorded at Pt(111)|Aciplex interfaces. For the Pt|ionomer interfaces prepared using the same drying temperature, the ORR activity decreases in the order of

Pt(111)|D72 > Pt(111)|Aciplex > Pt(111)|Nafion (Fig.3b, S4b), and also decreases with the drying temperature.

To unveil how the intrinsic ORR activity changes with the introduction of proton exchange ionomer membrane as well as with the drying temperature, the kinetic current for ORR is estimated using the j-E curves and the Koutecky-Levich equation (Fig.5a).[43] From Fig.5a, a significant poisoning effect on ORR by the sulfonate adsorbate can be observed. This effect is similar to that for ORR at Pt(111) in 0.1 M $HClO_4$ + x M H_2SO_4 (Fig.S1c). In order to determine the actual intrinsic ORR activity, the estimated kinetic current at 0.9 V for ORR is further normalized to the free available active sites on Pt(111) surface. An initial normalization has been done by assuming that the sites covered by adsorbed sulfonate do not participate in the ORR at this potential, since the activity for the ORR at this potential of the Pt(111) electrode for high sulfate concentrations is negligible (Fig.5b, Nj_{k1}). Here it is assumed that the sulfonate bonding configuration does not change with the drying temperature and occupies three Pt sites. A second normalization has been performed assuming that the diminution of the H_{upd} charge is related to the blocking of active sites by the polymer chain. Thus, the active area has been corrected both by the sites blocked by sulfonate and the polymer chain (Fig.5c, Nj_{k2}). The normalized j_k for ORR at 0.9 V on Pt(111)|X interface prepared using different drying temperatures are shown in Fig.5b and Fig.5c. For the sake of comparison, similar data from Pt(111)|0.1 M $HClO_4$+ x M H_2SO_4 and Pt|0.05 M H_2SO_4 interfaces are also included. From Fig.5b and Fig.5c, it is seen that the intrinsic ORR activity for the free sites on Pt(111)|ionomer interfaces is significantly higher than those at Pt(111)|0.1 M $HClO_4$+ x M H_2SO_4 or at Pt|0.05 M H_2SO_4 interface. For the three ionomers, the intrinsic ORR activity decreases in the order of Pt(111)|D72 > Pt(111)|Aciplex > Pt(111)|Nafion (Fig.S5). The results suggest that the ORR intrinsic activity depends on the side-chain structure of the ionomer. The intrinsic ORR activity of Pt(111)|D72 is superior to that of Pt(111)|Aciplex due to its shorter side chain, but the gap between them decreases gradually as the drying temperature increases. However, the intrinsic ORR activity of Pt(111)|Aciplex is better than Pt(111)|Nafion although the length of their side chains is nearly the same. The reason for this phenomenon is that the ether group within the Nafion's side chain is hydrophilic, which makes a difference from that of $(-CF_2-)_n$ groups in the side chain of Aciplex (Fig.1).

All these indicate that the local humidity degree within the proton exchange ionomer has a positive impact on ORR kinetics, which probably correlates with the smaller OH_{ad} coverage and positive shift of current wave for OH_{ad} formation (Fig.2, Fig. S2, S3).[44, 45] This is in good agreement with the previous finding that ORR kinetics at Pt is mainly limited by the thermodynamic equilibrium potential of water oxidation to OH_{ad}.[46-48] Furthermore, the lower the drying temperature is, the slightly higher kinetic current for ORR is obtained. The important conclusion of these findings regarding the local environment at the interface determines the ORR activity. Thus, the desired polymer materials should have a negligible poisoning effect by the sulfonate group along with a positive effect from the low chemical potential of water within the ionomer. Reducing the drying temperature for preparing the Pt(111)|ionomers interface as well as using ionomers with shorter side-chain may help realize such a goal.

Inspired by these ideas, we have prepared Pt(111)|Aciplex, Pt(111)|D72 (Fig.1), and Pt(111)|PTFE interface with ionomer or PTFE thickness of ca. 100 nm using a drying temperature of 55°C. The base CVs and j-E curves for ORR at such interfaces are shown in Fig.6. From the CVs we see that with the introduction of the Aciplex or D72 ionomers with a drying temperature of 55 °C, the adsorption of the sulfonate group is negligibly small, while the current waves for both the H_{UPD} and OH_{ad} adsorption are slightly inhibited due to the introduction of PTFE. Fig.6c and 6d show the ORR polarization curves recorded at Pt(111)|Aciplex, Pt(111)|D72 or Pt(111)|PTFE electrode interface. From these curves as well as the magnification of the kinetic region shown in the inset, it can be observed that the ORR performance at such interface is close to (or even slightly better than) the bare Pt(111) electrode. The normalized j_k at 0.9 V of Pt(111)|PTFE, Pt(111)|D72, and Pt(111)|Aciplex model interface prepared by drying at 55 °C are also included in Fig.5b and Fig.5c. It clearly shows that the intrinsic ORR activity decreases in the order of Pt(111)|PTFE > Pt(111)|D72 > Pt(111)|Aciplex > bare Pt(111). Furthermore, it is found that the ORR performance of Pt(111)|D72 film electrode is even superior to Pt(111)|Aciplex film electrode although the sulfonate poisoning effect (as indicated from their base CVs) is almost the same. This also correlates well with the slightly smaller current wave for OH_{ad} formation (Fig.6b). All these confirm our conjecture that the enhanced ORR kinetics is the result of the beneficial effect of the low chemical potential of water at Pt(111)|ionomer or Pt(111)|PTFE interface.

Besides the change of the chemical potential of water within the ionomer, it should be highlighted that the slight drop of the current wave for peak I and the positive shift of peak II for OH_{ad} formation as well as the decrease of intrinsic ORR activity with the increase of drying temperature from 120 °C to 195 °C for preparing the Pt|ionomer model interfaces may also, at least partly, correlate to a change of sulfonate adsorption (as indicated the negative shift of onset potential for sulfonate adsorption) as well as it induced electric double layer effect.[29] The potential of zero charge (PZC) of Pt(111) is 0.3 V vs SHE in the absence of specifically adsorbed anions, so that, at the potentials where the ORR is in the kinetic or kinetic-mass transport mixed controlled potential region, the Pt(111) surface is depleted of free electrons (positively charged).[34] The more negative the sulfonate adsorption potential is, the slightly more negative the PZC for the Pt(111)|ionomer interface is.[49-54] This renders that the electric potential at the Helmholtz plane (HP) is more positive, while the proton concentration at the HP is smaller due to electrostatic repulsion (Fig.S6). In addition to the lower water chemical potential within the ionomer, the more positive electric potential at the HP also renders the electrochemical driving force for water oxidation towards more positive potentials (Fig.S6).[29, 30, 34, 55] In contrast, for ORR, the positive shift of the electric potential at the HP increases the driving force for ORR. However, as the proton concentration at the HP decreases, the effect of the drop of proton concentration dominates, also leading to an adverse effect on ORR kinetics. (more detail information in SI)

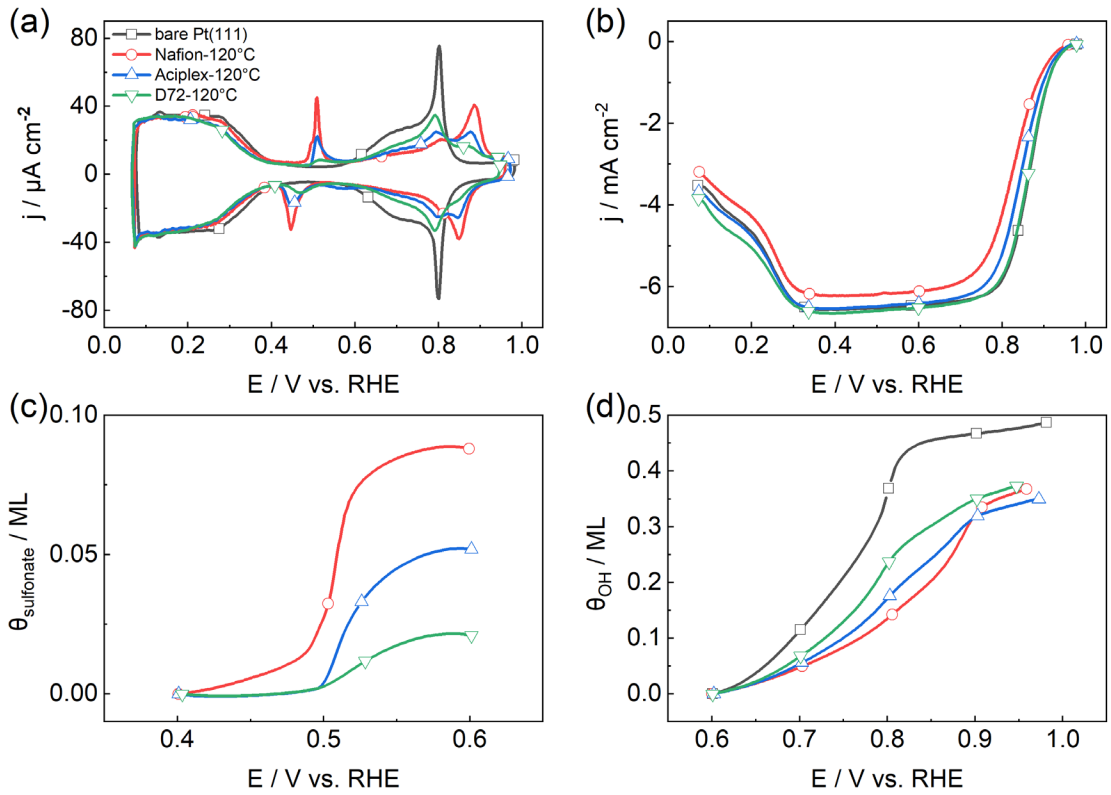

Fig. 3 (a) CVs for Pt(111)|X (Nafion, Aciplex, D72) film electrodes with a thickness of ca. 100 nm prepared with 120°C. (b) Polarization curves for ORR recorded in the positive scan. (c) Coverage of sulfonate ($\theta_{sulfonate}$, after the correction of double-layer charging current) as a function of the applied potential. (d) Coverage of adsorbed OH (θ_{OHad}, after the correction of double-layer charging current) as a function of the applied potential. For comparison, the base CV and the j-E curve for ORR at bare Pt(111) in 0.1 M $HClO_4$ are also included in (a) and (b). Electrolyte: 0.1 M $HClO_4$, scan rate: 50 mV/s. For ORR experiments, the rotation speed is 1600 rpm.

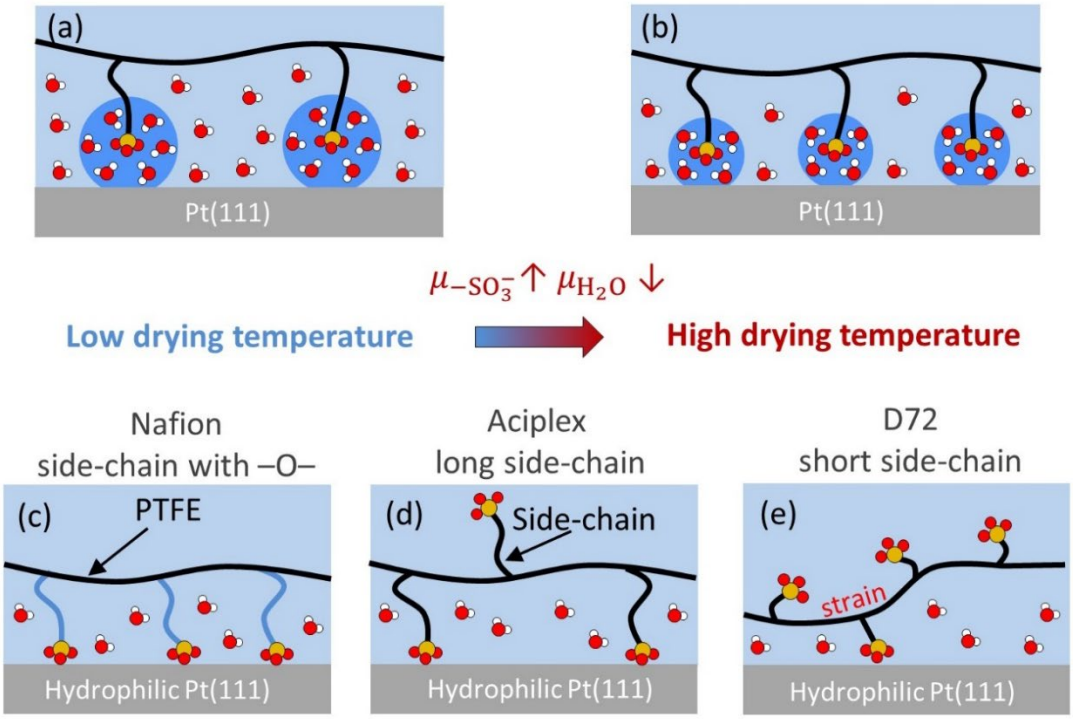

Fig. 4 Possible adsorption structure of ionomers on Pt(111) electrode: (a) low drying temperature, (b) high drying temperature, (c)Nafion, (d)Aciplex, and (e)D72.

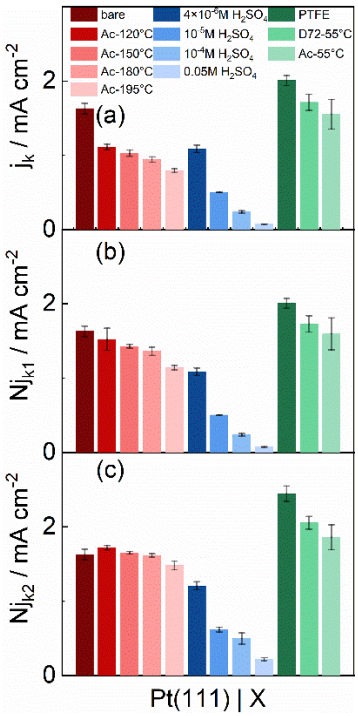

Fig. 5 (a) Kinetic current j_k at 0.9 V after correcting with the surface area of Pt(111)|X (Aciplex, D72, PTFE) film electrode prepared with different temperatures in 0.05 M H_2SO_4, x M H_2SO_4+0.1 M $HClO_4$

(X=4×10^{-6}, 10^{-5}, 10^{-4}). (b) Corresponding normalized j_{k1} at 0.9 V after correcting with the active area (geometric area minus sulfonate blocking area). (c) Corresponding normalized j_{k2} at 0.9 V after correcting with the active area (geometric area minus sulfonate blocking area minus PTFE blocking area). For comparison, j_k and normalized j_k of bare Pt(111) in 0.1 M $HClO_4$ are also included.

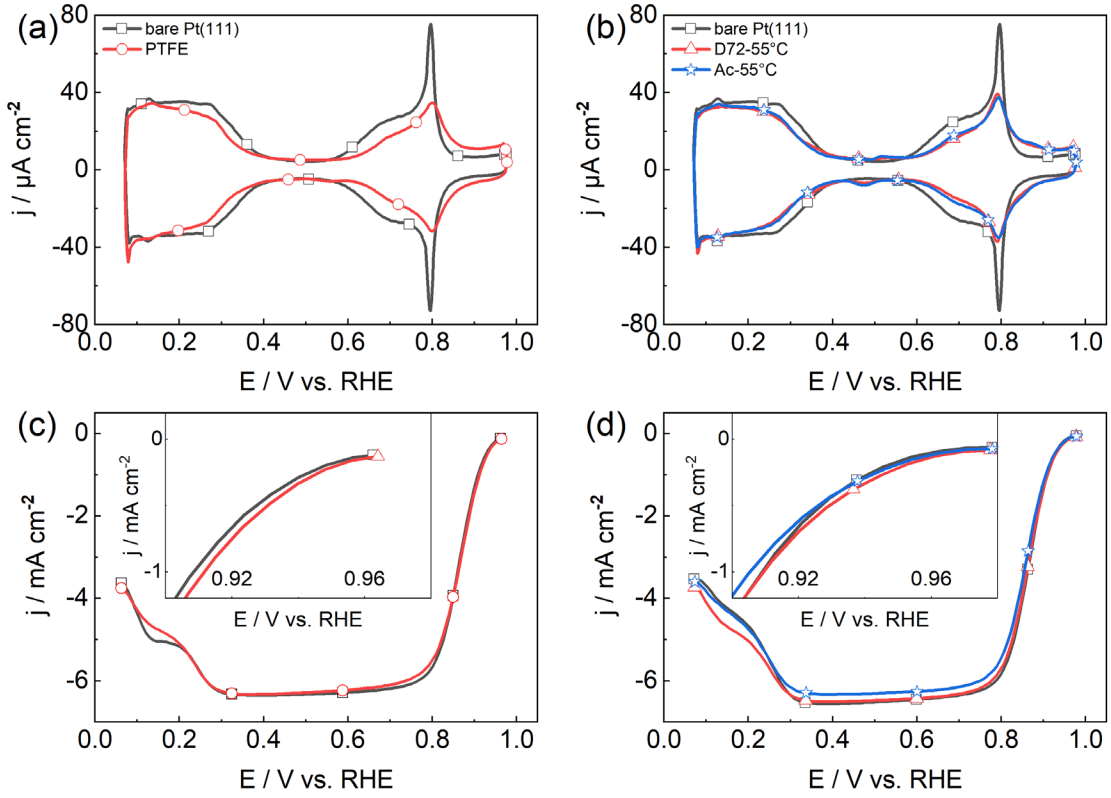

Fig. 6 CVs for (a) Pt(111)|PTFE film electrode and (b) Pt(111)|ionomer (D72, Aciplex) film electrodes with a thickness of ca. 100 nm prepared with 55°C. Polarization curves for ORR recorded in the positive scan for (c) Pt(111)|PTFE film electrode and (d) Pt(111)|D72 and Pt(111)|Aciplex film electrodes. Inset: detailed view of the kinetic region of ORR polarization curves. For comparison, the base CV and the j-E curve for ORR at bare Pt(111) in 0.1 M $HClO_4$ are also included. Electrolyte: 0.1 M $HClO_4$, scan rate: 50 mV/s. For ORR experiments, the rotation speed is 1600 rpm.

4. Conclusion

The impact of side-chain structure and length as well as their humidity degree on the sulfonate and OH adsorption at Pt(111)|ionomer interfaces on ORR kinetics are investigated systematically by using Nafion, Aciplex, and D72 as proton exchange ionomers. Control studies at Pt(111)|0.1 M $HClO_4$ with different concentrations of H_2SO_4 and at Pt(111)|PTFE interface have

also been carried out. The results reveal that, under otherwise identical conditions, ORR currents decrease in the order of Pt(111)|D72 > Pt|Aciplex > Pt(111)|Nafion, which is just opposite to the trend for 1) the sulfonate adsorption strength; 2) the positive shift extent of current wave for OH_{ad} adsorption; 3) the reduction of OH_{ad} formation current and charge at lower potentials.

Higher intrinsic ORR activity on the free sites is observed after proper correction of the blocking effect of Pt active sites by sulfonate adsorption and the PTFE skeleton. The activity decreases in the order of Pt(111)|PTFE > Pt(111)|D72 > Pt|Aciplex > Pt(111)|Nafion. According to the mixed potential effect, the smaller water activity at Pt(111)|ionomer (or PTFE) interfaces when compared to that of the Pt(111)|0.1 M $HClO_4$ interface is found to be the origin for the positive shift of adsorption peaks for OH_{ad} and the enhanced ORR kinetics. The lower onset potential for sulfonate adsorption at Pt|X (Nafion, Aciplex, D72) films prepared using higher drying temperatures is also explained by a reduction of the ionomer hydration extent, which increases the chemical potential of the sulfonate group within the ionomer. The latter also induces an additional electrostatic double-layer effect, which consequently alters ORR kinetics by changing the driving force for ORR and proton concentration in the reaction plane.

Observations herein disclose the critical importance of water activity and the electrostatic double-layer effect on the activity of the fuel cell-related reactions. Furthermore, our work provides strategies for the construction of Pt|ionomer interfaces in PEFCs to mitigate the adverse effect of sulfonate adsorption, choosing low annealing temperatures and ionomers with short side-chain. These strategies are universal and can provide guidelines in designing catalyst layers for the development of more efficient PEFCs, together with the development of advanced catalysts.

Acknowledgments

This work was supported by the National Natural Science Foundation of China (no. 21972131, 21832004). E.H. gratefully acknowledges the International Professorship by USTC and financial support from the Ministerio de Ciencia e Innovación (project PID2022-137350NB-I00).

5. Reference:

[1] K. Kodama, T. Nagai, A. Kuwaki, R. Jinnouchi, Y. Morimoto, Challenges in applying highly active Pt-based nanostructured catalysts for oxygen reduction reactions to fuel cell vehicles, Nat. Nanotechnol., 16 (2021) 140-147.

[2] J. Fan, M. Chen, Z. Zhao, Z. Zhang, S. Ye, S. Xu, H. Wang, H. Li, Bridging the gap between highly active oxygen reduction reaction catalysts and effective catalyst layers for proton exchange

membrane fuel cells, Nat. Energy, 6 (2021) 475-486.
[3] K. Jiao, J. Xuan, Q. Du, Z. Bao, B. Xie, B. Wang, Y. Zhao, L. Fan, H. Wang, Z. Hou, S. Huo, N.P. Brandon, Y. Yin, M.D. Guiver, Designing the next generation of proton-exchange membrane fuel cells, Nature, 595 (2021) 361-369.
[4] C.-L. Yang, L.-N. Wang, P. Yin, J. Liu, M.-X. Chen, Q.-Q. Yan, Z.-S. Wang, S.-L. Xu, S.-Q. Chu, C. Cui, H. Ju, J. Zhu, Y. Lin, J. Shui, H.-W. Liang, Sulfur-anchoring synthesis of platinum intermetallic nanoparticle catalysts for fuel cells, Science, 374 (2021) 459-464.
[5] X.X. Wang, M.T. Swihart, G. Wu, Achievements, challenges and perspectives on cathode catalysts in proton exchange membrane fuel cells for transportation, Nat. Catal., 2 (2019) 578-589.
[6] Z. Ma, Z.P. Cano, A. Yu, Z. Chen, G. Jiang, X. Fu, L. Yang, T. Wu, Z. Bai, J. Lu, Enhancing Oxygen Reduction Activity of Pt-based Electrocatalysts: From Theoretical Mechanisms to Practical Methods, Angew. Chem. Int. Ed., 59 (2020) 18334-18348.
[7] S. Ott, A. Orfanidi, H. Schmies, B. Anke, H.N. Nong, J. Hübner, U. Gernert, M. Gliech, M. Lerch, P. Strasser, Ionomer distribution control in porous carbon-supported catalyst layers for high-power and low Pt-loaded proton exchange membrane fuel cells, Nat. Mater., 19 (2020) 77-85.
[8] Y. Sun, S. Polani, F. Luo, S. Ott, P. Strasser, F. Dionigi, Advancements in cathode catalyst and cathode layer design for proton exchange membrane fuel cells, Nat. Commun., 12 (2021) 5984.
[9] C.-Y. Li, J.-B. Le, Y.-H. Wang, S. Chen, Z.-L. Yang, J.-F. Li, J. Cheng, Z.-Q. Tian, In situ probing electrified interfacial water structures at atomically flat surfaces, Nat. Mater., 18 (2019) 697-701.
[10] A. Kusoglu, A.Z. Weber, New Insights into Perfluorinated Sulfonic-Acid Ionomers, Chem. Rev., 117 (2017) 987-1104.
[11] X. Yan, Z. Xu, S. Yuan, A. Han, Y. Shen, X. Cheng, Y. Liang, S. Shen, J. Zhang, Structural and transport properties of ultrathin perfluorosulfonic acid ionomer film in proton exchange membrane fuel cell catalyst layer: A review, J. Power Sources, 536 (2022) 231523.
[12] K. Shinozaki, Y. Morimoto, B.S. Pivovar, S.S. Kocha, Suppression of oxygen reduction reaction activity on Pt-based electrocatalysts from ionomer incorporation, J. Power Sources, 325 (2016) 745-751.
[13] J. Tymoczko, F. Calle-Vallejo, V. Colic, M.T.M. Koper, W. Schuhmann, A.S. Bandarenka, Oxygen Reduction at a Cu-Modified Pt(111) Model Electrocatalyst in Contact with Nafion Polymer, ACS Catal., 4 (2014) 3772-3778.
[14] R. Subbaraman, D. Strmcnik, A.P. Paulikas, V.R. Stamenkovic, N.M. Markovic, Oxygen Reduction Reaction at Three-Phase Interfaces, ChemPhysChem, 11 (2010) 2825-2833.
[15] R. Subbaraman, D. Strmcnik, V. Stamenkovic, N.M. Markovic, Three Phase Interfaces at Electrified Metal-Solid Electrolyte Systems 1. Study of the Pt(hkl)-Nafion Interface, J. Phys. Chem. C, 114 (2010) 8414-8422.
[16] M. Ahmed, D. Morgan, G.A. Attard, E. Wright, D. Thompsett, J. Sharman, Unprecedented Structural Sensitivity toward Average Terrace Width: Nafion Adsorption at Pt{hkl} Electrodes, The Journal of Physical Chemistry C, 115 (2011) 17020-17027.
[17] M. Luo, M.T.M. Koper, A kinetic descriptor for the electrolyte effect on the oxygen reduction kinetics on Pt(111), Nat. Catal., 5 (2022) 615-623.
[18] K. Kodama, K. Motobayashi, A. Shinohara, N. Hasegawa, K. Kudo, R. Jinnouchi, M. Osawa, Y. Morimoto, Effect of the Side-Chain Structure of Perfluoro-Sulfonic Acid Ionomers on the Oxygen Reduction Reaction on the Surface of Pt, ACS Catal., 8 (2018) 694-700.
[19] K. Kodama, A. Shinohara, N. Hasegawa, K. Shinozaki, R. Jinnouchi, T. Suzuki, T. Hatanaka, Y.

Morimoto, Catalyst Poisoning Property of Sulfonimide Acid Ionomer on Pt (111) Surface, J. Electrochem. Soc., 161 (2014) F649-F652.
[20] K. Kodama, R. Jinnouchi, T. Suzuki, H. Murata, T. Hatanaka, Y. Morimoto, Increase in adsorptivity of sulfonate anions on Pt (111) surface with drying of ionomer, Electrochem. Commun., 36 (2013) 26-28.
[21] R. Jinnouchi, K. Kudo, K. Kodama, N. Kitano, T. Suzuki, S. Minami, K. Shinozaki, N. Hasegawa, A. Shinohara, The role of oxygen-permeable ionomer for polymer electrolyte fuel cells, Nat. Commun., 12 (2021) 4956-4964.
[22] Y. Li, S. Intikhab, A. Malkani, B. Xu, J. Snyder, Ionic Liquid Additives for the Mitigation of Nafion Specific Adsorption on Platinum, ACS Catal., 10 (2020) 7691-7698.
[23] K. Kodama, K. Motobayashi, Adsorption of ionomer and ionic liquid on model Pt catalysts for polymer electrolyte fuel cells, Electrochem. Sci. Adv., n/a (2022) e2100183.
[24] T. Kumeda, N. Hoshi, M. Nakamura, Effect of Hydrophobic Cations on the Inhibitors for the Oxygen Reduction Reaction on Anions and Ionomers Adsorbed on Single-Crystal Pt Electrodes, ACS Appl. Mater. Interfaces, 13 (2021) 15866-15871.
[25] F. Chen, S. Chen, A. Wang, M. Wang, L. Guo, Z. Wei, Blocking the sulfonate group in Nafion to unlock platinum's activity in membrane electrode assemblies, Nat. Catal., 6 (2023) 392-401.
[26] Q. Zhang, S. Dong, P. Shao, Y. Zhu, Z. Mu, D. Sheng, T. Zhang, X. Jiang, R. Shao, Z. Ren, J. Xie, X. Feng, B. Wang, Covalent organic framework–based porous ionomers for high-performance fuel cells, Science, 378 (2022) 181-186.
[27] K. Kunimatsu, B. Bae, K. Miyatake, H. Uchida, M. Watanabe, ATR-FTIR Study of Water in Nafion Membrane Combined with Proton Conductivity Measurements during Hydration/Dehydration Cycle, The Journal of Physical Chemistry B, 115 (2011) 4315-4321.
[28] B. Garlyyev, S. Xue, M.D. Pohl, D. Reinisch, A.S. Bandarenka, Oxygen Electroreduction at High-Index Pt Electrodes in Alkaline Electrolytes: A Decisive Role of the Alkali Metal Cations, ACS Omega, 3 (2018) 15325-15331.
[29] W. Chen, L.-L. Zhang, Z. Wei, M.-K. Zhang, J. Cai, Y. Chen, The Double Layer Effect with Specifically Adsorbed Anions and Its Promotion Toward Electrocatalytic Reactions, Phys. Chem. Chem. Phys., 25 (2023) 8317-8330.
[30] M.-K. Zhang, J. Cai, Y.-X. Chen, On the electrode charge at the metal/solution interface with specific adsorption, Curr. Opin. Electrochem., 36 (2022) 101161-101175.
[31] J. Clavilier, The role of anion on the electrochemical behaviour of a {111} platinum surface; an unusual splitting of the voltammogram in the hydrogen region, J. Electroanal. Chem. Interfacial Electrochem., 107 (1980) 211-216.
[32] J. Clavilier, R. Faure, G. Guinet, R. Durand, Preparation of monocrystalline Pt microelectrodes and electrochemical study of the plane surfaces cut in the direction of the {111} and {110} planes, J. Electroanal. Chem. Interfacial Electrochem., 107 (1980) 205-209.
[33] J. Clavilier, D. Armand, S.G. Sun, M. Petit, Electrochemical adsorption behaviour of platinum stepped surfaces in sulphuric acid solutions, J. Electroanal. Chem. Interfacial Electrochem., 205 (1986) 267-277.
[34] V. Briega-Martos, E. Herrero, J.M. Feliu, Effect of pH and Water Structure on the Oxygen Reduction Reaction on platinum electrodes, Electrochim. Acta, 241 (2017) 497-509.
[35] N. Garcia-Araez, V. Climent, P. Rodriguez, J.M. Feliu, Thermodynamic analysis of (bi)sulphate adsorption on a Pt(111) electrode as a function of pH, Electrochim. Acta, 53 (2008) 6793-6806.

[36] J. Wei, Z.-d. He, W. Chen, Y.-X. Chen, E. Santos, W. Schmickler, Catalysis of hydrogen evolution on Pt(111) by absorbed hydrogen, The Journal of Chemical Physics, 155 (2021) 181101.
[37] A. Berná, V. Climent, J.M. Feliu, New understanding of the nature of OH adsorption on Pt(111) electrodes, Electrochem. Commun., 9 (2007) 2789-2794.
[38] R. Wang, T. Tian, Z. Wan, F. Zhou, L.I. Shang, J. Tan, M. Pan, Effect of trifluoromethanesulfonic acid on the ORR activity of Pt in acid medium, Int. J. Electrochem. Sci., 14 (2019) 1809-1816.
[39] Z. Wei, M.K. Zhang, B.Q. Zhu, M.L. Xu, J. Lei, H. Tang, J. Cai, Y.-X. Chen, Effect of pH on Sulfate Adsorption on the Pd(111) Electrode, The Journal of Physical Chemistry C, 126 (2022) 3891-3902.
[40] H.F.M. Mohamed, S. Kuroda, Y. Kobayashi, N. Oshima, R. Suzuki, A. Ohira, Possible presence of hydrophilic SO3H nanoclusters on the surface of dry ultrathin Nafion® films: a positron annihilation study, Phys. Chem. Chem. Phys., 15 (2013) 1518-1525.
[41] M. Tesfaye, A.N. MacDonald, P.J. Dudenas, A. Kusoglu, A.Z. Weber, Exploring substrate/ionomer interaction under oxidizing and reducing environments, Electrochem. Commun., 87 (2018) 86-90.
[42] A. Ohira, S. Kuroda, H.F.M. Mohamed, B. Tavernier, Effect of interface on surface morphology and proton conduction of polymer electrolyte thin films, Phys. Chem. Chem. Phys., 15 (2013) 11494-11500.
[43] A. Bard, L. Faulkner, J. Leddy, C. Zoski, Electrochemical methods: fundamentals and applications, vol 2 John Wiley & Sons, New York, NY.[Google Scholar], (1980).
[44] J. Staszak-Jirkovský, R. Subbaraman, D. Strmcnik, K.L. Harrison, C.E. Diesendruck, R. Assary, O. Frank, L. Kobr, G.K.H. Wiberg, B. Genorio, J.G. Connell, P.P. Lopes, V.R. Stamenkovic, L. Curtiss, J.S. Moore, K.R. Zavadil, N.M. Markovic, Water as a Promoter and Catalyst for Dioxygen Electrochemistry in Aqueous and Organic Media, ACS Catal., 5 (2015) 6600-6607.
[45] Y. Yang, R.G. Agarwal, P. Hutchison, R. Rizo, A.V. Soudackov, X. Lu, E. Herrero, J.M. Feliu, S. Hammes-Schiffer, J.M. Mayer, H.D. Abruña, Inverse kinetic isotope effects in the oxygen reduction reaction at platinum single crystals, Nat. Chem., 15 (2023) 271-277.
[46] M.F. Li, L.W. Liao, D.F. Yuan, D. Mei, Y.-X. Chen, pH effect on oxygen reduction reaction at Pt(111) electrode, Electrochim. Acta, 110 (2013) 780-789.
[47] W. Chen, J. Huang, J. Wei, D. Zhou, J. Cai, Z.-D. He, Y.-X. Chen, Origins of high onset overpotential of oxygen reduction reaction at Pt-based electrocatalysts: A mini review, Electrochem. Commun., 96 (2018) 71-76.
[48] H.S. Casalongue, S. Kaya, V. Viswanathan, D.J. Miller, D. Friebel, H.A. Hansen, J.K. Nørskov, A. Nilsson, H. Ogasawara, Direct observation of the oxygenated species during oxygen reduction on a platinum fuel cell cathode, Nat. Commun., 4 (2013) 2817.
[49] D.J. Barclay, Chemical softness and specific adsorption at electrodes, J. Electroanal. Chem. Interfacial Electrochem., 19 (1968) 318-321.
[50] B.E. Conway, The solvation factor in specificity of ion adsorption at electrodes, Electrochim. Acta, 40 (1995) 1501-1512.
[51] B.E. Conway, The role of solvation, complementary to electronic effects, in specific adsorption of ions at electrodes, Solid State Ionics, 94 (1997) 165-170.
[52] O.M. Magnussen, Ordered Anion Adlayers on Metal Electrode Surfaces, Chem. Rev., 102 (2002) 679-726.
[53] W. Schmickler, The Effect of Weak Adsorption on the Double Layer Capacitance, ChemElectroChem, 8 (2021) 4218-4222.

[54] K. Ojha, K. Doblhoff-Dier, M.T.M. Koper, Double-layer structure of the Pt(111)–aqueous electrolyte interface, PNAS, 119 (2022) 1-9.
[55] X. Ding, D. Scieszka, S. Watzele, S. Xue, B. Garlyyev, R.W. Haid, A.S. Bandarenka, A Systematic Study of the Influence of Electrolyte Ions on the Electrode Activity, ChemElectroChem, 9 (2022) e202101088.